

## INVESTIGATION OF COUPLING STRENGTH AT NON-CENTRAL INTERACTION OF RAILCARS

A. O. Shvets'

UDC 629.463.028.31-046.32

*The strength of the coupling device under the action of operating loads with regard to the non-central interaction of two cars is defined. When longitudinal force is transmitted through the coupler, the points of its possible rotation can be either the upper ribs of the shank end surface or the upper ribs of the damping device body support surface. The tail part of the coupler is under conditions of eccentric compression (or tension) by the force, which is non-parallel to the longitudinal axis. Through any cross-section of the shank, transverse and longitudinal forces are transmitted, applied at a point far from the center of gravity of the section. Using the principle of addition of forces action, a dependence for the definition of the maximum normal stresses in the extreme fibers of the analyzed section of the shank of the coupler, the most distant from the main axis of inertia, has been obtained. The damage to the area of the coupler shank jumper and the bending of the shank in the horizontal and vertical planes, which occur during operation, are justified. Calculation methods make it possible to study the influence of eccentricities of longitudinal force application relative to the coupler axis and the difference of coupler axis levels in the analyzed sections on the magnitude of the compressive operating loads. Application of the obtained results will not only help to ensure the strength of the coupling devices, but will also ensure the freight cars' durability under conditions of increasing train weight and increasing train speed.*

**Keywords:** coupler, safety, freight car, strength, longitudinal forces.

**Introduction.** Increasing the speed and weight of freight trains are the most effective means of mastering the volume of traffic and further increasing rail traffic [1–3]. At the same time, the strength of traction and coupling devices must meet the large longitudinal forces that develop in trains of increased weight [4–7].

As is known, the strength and resource of the main load-bearing elements of railroad rolling stock are fundamental properties that determine their further successful operation for a long period of time. Estimation of these indicators is closely connected with ensuring of traffic safety requirements of the railroad transport. Therefore, the problem of scientific substantiation of estimation of dynamics characteristics, strength, and resource of bearing structures is important and urgent [8–10].

When designing high-speed cars, the following assumptions are used: increase in strength and operational reliability of the design, possibility of a more complete application of complex mechanization of loading and unloading operations, ensuring the preservation of cargoes which are transported in cars. Fulfillment of these requirements predetermines the need for extensive theoretical and experimental research, in particular when specifying the calculations of car design for strength and stiffness with regard to the action of shift loads and longitudinal forces in the train [11–13].

Longitudinal forces in trains sometimes reach a value exceeding the strength of car frames of some designs. Studies have shown that large values of impact and pulling forces are caused mainly by the following factors: abrupt

---

Dnipro National University of Railway Transport named after Academician V. Lazarian, Dnipro, Ukraine (angela\_Shvets@ua.fm, <http://orcid.org/0000-0002-8469-3902>). Translated from Problemy Mitsnosti, No. 2, pp. 77 – 87, March – April, 2022. Original article submitted June 1, 2021.

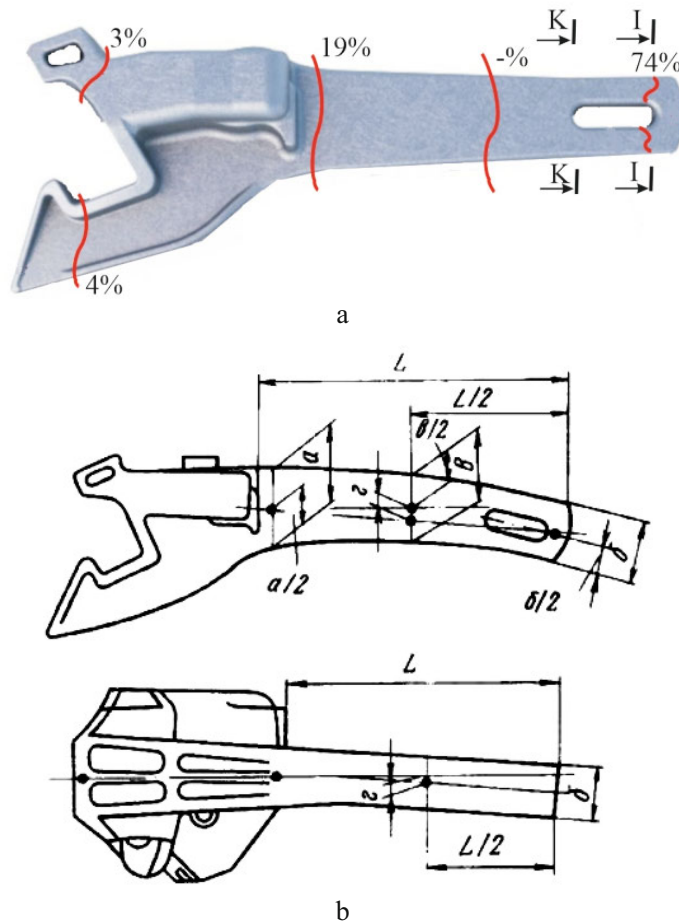


Fig. 1. Damage to the coupling device during operation: (a) distribution of failures over the section of the coupling body; (b) deformations of the coupling body. (Figures show the share of damage in %.)

train movement after stopping; pulling of partially compressed train, especially with fully extended tail part, which has cars with unreleased brakes; stopcock braking in the tail of train at low travel speed and compressed rolling stock at the beginning of braking [11].

The magnitude of forces, which are transmitted to the frame and other parts of the car by the shock-traction devices, depends on the effectiveness of the absorption devices and misalignment of the axles of the couplers of the neighboring cars. The correct positioning of the coupling device on the car frame is of great importance (prevention of the damping device misalignment and ensuring the central loading of the ridge beam) [14–17].

It was noted in [18] that about 74.3% of the total number of damages in the coupling device corresponded to the damages of the coupling shank jumper zone. The places of the most frequent damage in the coupler body are shown in Fig. 1. In addition, bending of the shank in the horizontal and vertical planes occurs during operation (Fig. 1b).

Considering the high cost of full-scale tests, it is necessary to focus on analytical methods and computer modeling when investigating the strength of wagons and individual components of rolling stock [11, 19–21].

The purpose of the work is to determine the strength of the coupling device under the action of operating loads, taking into account the non-central interaction of two cars.

**Analysis of Publications and Statement of the Problem.** Using 3D modeling systems (KOMPAS-3D, ANSYS, APM Winmachine, Solidworks, etc.) after building a 3D-model one can obtain not only the stress-strain state, inertial and mass characteristics but also the stiffness value at different types of loading of both individual car elements and the whole car [5–7, 21].

TABLE 1. Mechanical Properties of the Coupler Housing Material

Steel grade	Yield strength [ $\sigma_y$ ], MPa	Ultimate strength [ $\sigma_{ul}$ ], MPa	Relative elongation $\delta$ , %	Elastic modulus $E$ , GPa
25Kh2NML	700	800	12	210
20GFL (20G1FL)	350	540	18	210

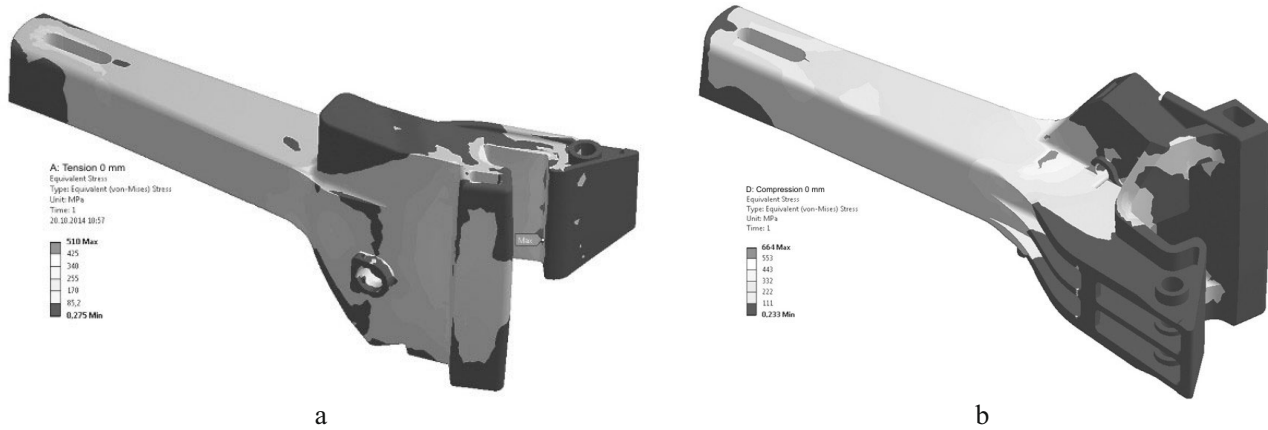


Fig. 2. Tensile (a) and compressive (b) equivalent stresses (in MPa) at the same height of the coupler axes.

In works [18, 22], the coupler body was calculated for the strength under the action on it of both tensile and compressive quasi-static and impact loads. The calculation scheme envisages the action of longitudinal forces on the stops at both ends of the car in the presence of a 100 mm difference in the height of coupling devices of interacting cars [14, 15, 17].

The calculations are performed using a software package that uses the finite element method. The finite-element model was created on the basis of the design documentation. The values of standard loads were selected according to the recommendations of the current normative documentation. Connections of the coupler body with the traction clamp wedge and with the thrust plate are implemented as supports of finite stiffness.

In the calculation scheme, the coupling housing is connected to the traction clamp wedge of the damping device (tensile forces) or to the thrust plate (compressive forces) by distributed elastic elements with finite stiffness. The coupling body is also supported on the centering beam by single-sided connections [18].

The strength was assessed according to the mechanical properties of the material of the coupler housing. The body of the coupling is made by casting with the following machining from steel 25Kh2NML [22] and 20GFL (20G1FL) [18]. The mechanical properties of the material of the coupler housing are given in Table 1.

Software complexes of three-dimensional modeling allow calculations of elements of complex configuration, variable magnitude, degree of dynamism, and points of application of design forces, which should be taken into account through the relative movements of couplers in operation, wear of their contour surface, and variable values of friction coefficients.

It follows from the results of calculations of the SA-3 coupler obtained in work [18] that working stresses in some areas exceed not only the yield stress but also the ultimate strength. This, as the operation shows, is the cause of formation of cracking at a single application of maximum longitudinal force and plastic deformations, which contribute to intensive nucleation of cracks of low-cycle fatigue.

Figure 2 shows the stress state at the application of longitudinal forces at the same height of the axes of the studied coupling devices made of steel 25Kh2NML [22].

During the tension of the coupler, the zones of maximum stress are located on the large tooth and at the joint of the head with the shank (Fig. 2a), and the compression stresses are located at the joint of the head with the shank (Fig. 2b).

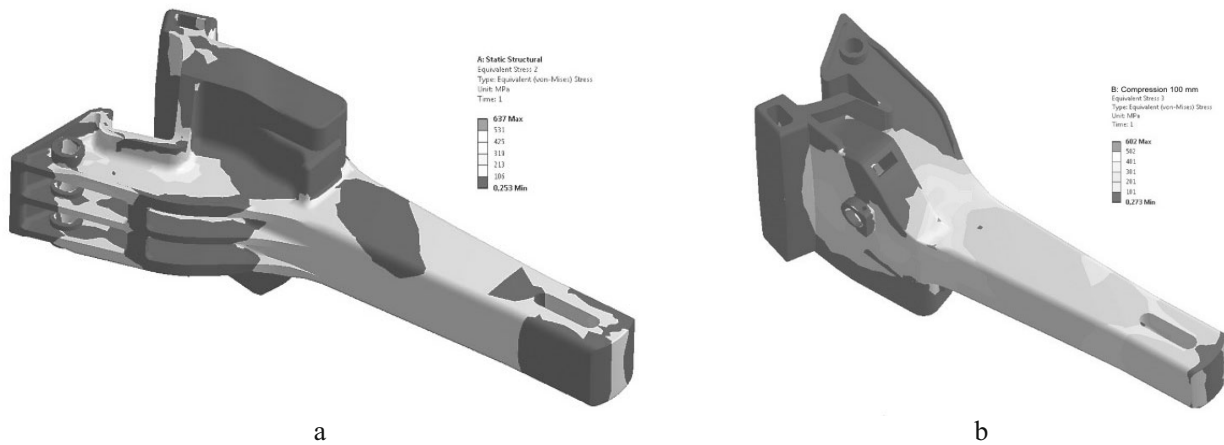


Fig. 3. Tensile (a) and compressive (b) equivalent stresses (in MPa) at displacement of the axis of the adjacent coupler 100 mm below the analyzed one.

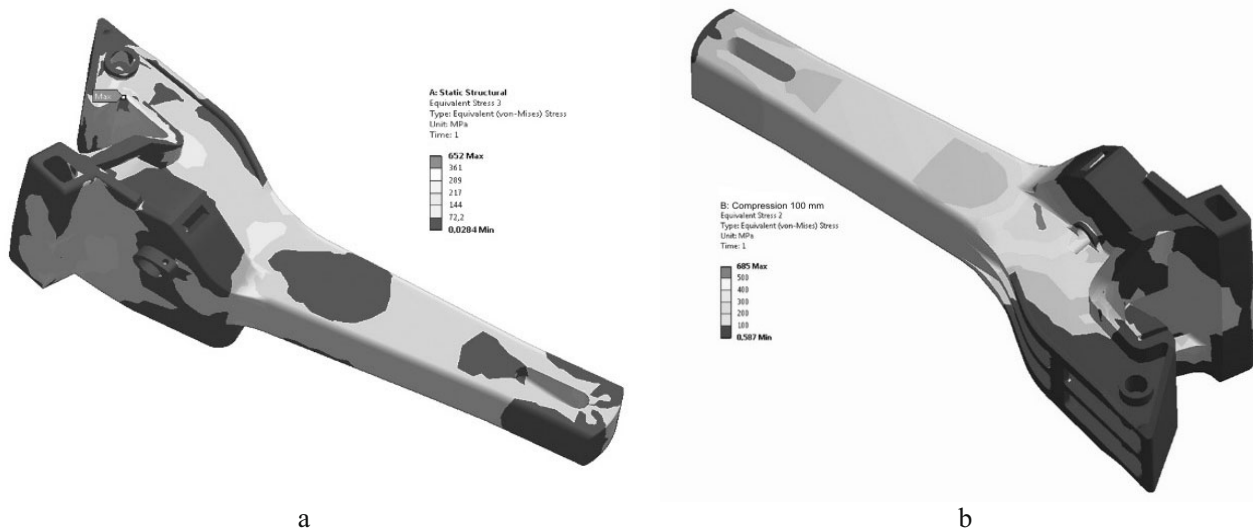


Fig. 4. Tensile (a) and compressive (b) equivalent stresses (in MPa) for the displacement of the axis of the adjacent coupler 100 mm higher than the analyzed one.

Figure 3 shows the stress state at the application of longitudinal forces in the presence of a 100 mm difference in the height of the coupling devices of the interacting cars (i.e., below the analyzed coupling).

As can be seen from Figs. 2b and 3b, the compressive force is transmitted to the coupler base plate at a point, and in case of warping of the cars in the train, this point of contact of the coupler tail part with the base plate can move across the crew. In the case of tensile longitudinal forces, the character of interaction changes significantly (Figs. 2 and 3a).

Figure 4 shows the stress state at the application of longitudinal forces in the presence of a 100 mm difference in the height of the coupling devices of the interacting cars (above the analyzed coupling).

According to the calculation results on the action of standard loads on the coupler body the highest values of stresses are 685 MPa (Fig. 4b), which is not above the yield stress limit of the material, equal to 700 MPa.

So, for all considered variants, during the tension of the coupling, the zones of maximum stresses are located on the large tooth and at the junction of the head with the shank, and during the compression – at the junction of the head with the shank. According to the results of the given research, the strength of the coupler housing at the action of the standard loads on it is provided.

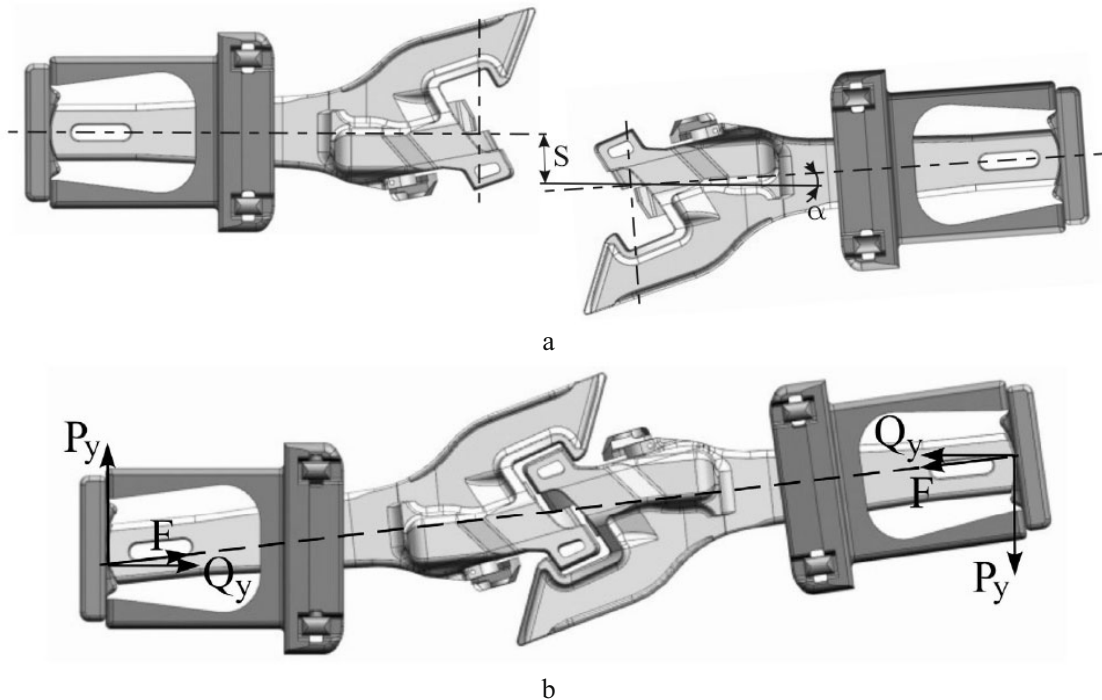


Fig. 5. Checking the coupling in the horizontal plane: (a) position of the couplers in the plan; (b) mutual position of the SA-3 couplers at the final moment of calculations.

The normative documentation recommends design diagrams of applying quasi-static longitudinal tensile or compressive forces in the vertical plane in case of non-central interaction of two neighboring cars with a difference in height of coupler axes of 0.1 m according to mode I (conditional safety mode) and 0.05 m – according to mode III (operational mode).

It is known that the automatic coupling device of cars should provide automatic coupling of rolling stock on straight and curved sections of the track, as well as keep the coupled state of the rolling stock during the movement on circular and S-like curves, marshalling hills, and ferry apparels [23].

A coupler misalignment in the horizontal plane occurs if the coupled cars or one of them is on a curved section of the track. The smaller the radius of the curve, the greater the deviation between the longitudinal axes of the couplings. These deviations significantly depend also on the length of the base and the cantilever part of the car. Axle offset in the horizontal direction, in which automatic coupling is provided, is allowed not more than 175 mm, which corresponds to the full width of the grip  $S$  with parallel axes of couplers for SA-3 without a guide wing (Fig. 5) [23].

The coupling check in the horizontal plane is carried out at the relative transverse displacement of the coupling axes in the horizontal direction  $\Delta S = \pm 160$  mm and the angle of rotation in the horizontal plane  $\alpha = \pm 4.5^\circ$ , as well as at  $\Delta S = \pm 40$  mm and  $\alpha = 8^\circ$  (Fig. 5a) [23].

Figure 5b shows the mutual location of the couplers in the calculations for the case  $\Delta S = 40$  mm,  $\alpha = 8^\circ$ , and  $\Delta h = 140$  mm (difference in the location of the axes of couplers in the vertical plane) [19]. You can see that compressive force is transferred to coupler base plate in the point, which moves in the horizontal plane across the crew, the true value of eccentricity for freight cars is mm [14, 15, 17].

An important feature of wagon running gears, which predetermines the increased lateral impact of wheel combs on the rail head during train braking, is the structural possibility of vertical and transverse horizontal movement of the body relative to the track axis [15, 17].

Through the presence of gaps between the ridges and the rail head, and spring, axlebox, and pivot-type assemblies, as well as the twisting motion of the crews, the eccentricities of the horizontal (Fig. 5b) and vertical

location of the coupling shanks relative to the nominal (design) longitudinal line of the coupling axles, the body and the couplings of the crews are located in the motion with some misalignment. When studying the train as an articulated-link system, it was also noted that two forms of stiffness loss are possible both in vertical and horizontal planes. The contact of the couplings is not over the entire surface of the interacting planes, but at individual contact points. When the coupling is tilted, the contact point between the shank and the wedge moves. In fact, the difference in height of the points, due to which the longitudinal force is transmitted with a difference in height of the couplings of 100 mm, is increased by the height of the coupler shank (130 mm) [24].

**Materials and Methods.** Significant vertical forces can act on the cantilever part of the car frame next to the longitudinal forces. The magnitude and direction of these forces depend on the longitudinal force, the nature of coupler interaction, the geometry of coupler parts, their physical and mechanical characteristics, the relative position of coupled cars and other factors. Since the previous calculations using the finite element method showed that the most unfavorable operating conditions of coupling devices, in terms of strength (Fig. 4, b), occur at compressive longitudinal loads, in the future the research is carried out exactly for this mode of interaction.

According to the normative documentation in case of non-central interaction of the coupling devices of two cars on the consoles of their bodies there are additional vertical forces  $P$ , which are determined by the formula

$$P = F \frac{e}{b} = F \frac{\Delta h_a}{2a_c}, \quad (1)$$

where  $F$  is the calculated longitudinal force (MN),  $e = \Delta h_a$  is the difference in the levels of the axes of coupled couplers (m), and  $b = 2a_c$  is the length of the rigid bar formed by two coupled couplers behind the conditional joints at the points of support on the cars A i B, or the doubled length of the coupling body from the coupling axis to the end of the shank (m).

When determining additional vertical forces in the case of non-central interaction of couplers of two cars according to the current normative documentation, only the difference of axle levels of coupled couplers is taken into account. However, the SA-3 (SA-3M) coupler has flat vertical surfaces of 160 mm in the coupling contour, which are located symmetrically to the longitudinal axis of the coupler at 80 mm upwards and downwards. Longitudinal forces are transmitted from one coupler to the other through these working surfaces. Since the working surfaces are planes, the resultant elementary contact forces, which are equal to their sum, can be transmitted through any point in the collision zone of the surfaces [18, 22, 24].

The longitudinal compressive force is transmitted through the end face of the coupler shank to the thrust plate, and the tensile force (traction force) is transmitted to the traction clamp wedge. In both cases the forces are transmitted through cylindrical surfaces, the axes of which are vertical. So, the resultant force, which is equal to the sum of elementary contact forces at the points of collision of the coupler shank with the thrust plate or the traction clamp wedge, can pass through any point of the vertical area of their surfaces collision [14, 15, 17].

There are three possible ways of coupler interaction in operation: no collision with the centering beams; one coupler collides with the centering beam, the second coupler or both couplers collide with the centering beams.

The first option, as a rule, takes place when couplers are placed on a car with sag. In this case, when the longitudinal force is applied, the couplings are lifted and have no contact with the centering beams. If the longitudinal axis of couplers is deflected upwards from the horizontal, the second and third options of coupler interaction are possible. Under this condition, additional vertical forces act between the centering beams and the coupling devices.

Let's consider the first variant of coupler interaction. When transmitting longitudinal force, the points of possible turn of the coupler can be the upper ribs of the end surface of the tail section (Figs. 3b and 4b), or the upper ribs of the supporting surface of the damper housing. If we neglect the longitudinal forces of inertia, taking into account their small magnitude compared to the longitudinal forces, which are transmitted through the coupler, we can assume that the couplers are in equilibrium under the action of external forces. Assume that the force  $F$ , which is transmitted through the coupler, is directed along the line  $A-A$  both in the vertical (Fig. 6) and in the horizontal plane

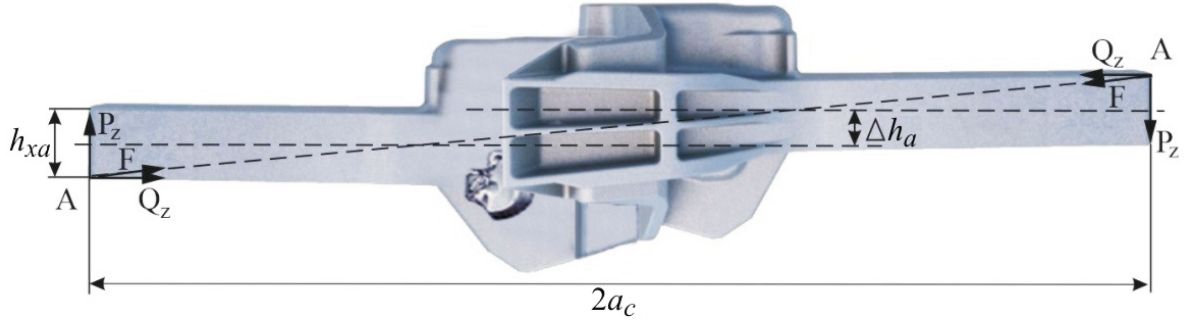


Fig. 6. Longitudinal forces that are transmitted through the coupler in the vertical plane.

(Fig. 5b). Let us decompose the force into horizontal (longitudinal)  $Q_z$ ,  $Q_y$  and vertical  $P_z$ ,  $P_y$  forces. In this type of interaction, the deformation energy is perceived exclusively by the coupler body.

The tail end of the coupling is under off-center compression (or tension) by a force, which is non-parallel to the longitudinal axis. Through an arbitrary cross-section of the shank there are transverse ( $P_z$ ,  $P_y$ ) and longitudinal forces ( $Q_z$ ,  $Q_y$ ) applied at a point distant from the center of gravity of the cross-section. The force acting on the couplers can be replaced by the normal force, which is applied at the center of gravity of the section, and the bending moments in the vertical  $M_z(x)$  and horizontal  $M_y(x)$  planes.

$$M_z = \frac{h_{xa}(x - a_c) + \Delta h_a x}{2a_c} F, \quad (2)$$

$$M_y = \frac{e_y(a_c - x)}{a_c} F. \quad (3)$$

According to the design documentation in sections  $I-I$  (opening under the wedge of the traction clamp,  $l=91.3$  cm) and  $K-K$  ( $l=80$  cm) the longitudinal force will form an additional bending moment due to eccentric compression of parts of the wedge of the traction clamp

$$M'_y = \frac{e_y(a_3 - x) \mp e'_y a_c}{2a_c} F, \quad (4)$$

where  $e_y$  and  $e'_y$  are eccentricities of the longitudinal force relative to the axis of the coupler in the analyzed sections  $I-I$  and  $K-K$  (for section  $I-I$   $e'_y = 4.15$  cm, for section  $K-K$   $e'_y = 4.39$  cm),  $h_{xa}$  is the height of the coupler tail, and  $x$  is the distance between the end surface of the coupler shank and the analyzed section.

Using the principle of superposition of forces, let's find the maximum normal stresses in the outermost fibers of the analyzed section of the coupling shank, farthest from the main axis of inertia

$$\sigma = \frac{F}{A_x} \pm \frac{M_z(x)}{W_z(x)} \pm \frac{M_y(x)}{W_y(x)}, \quad (5)$$

where  $W_z(x)$  and  $W_y(x)$  are the moments of resistance of the section of the coupler shank in the appropriate planes and  $A_x$  is the cross-sectional area of the coupler shank (Fig. 7).

As the longitudinal force increases, the stresses in the weak sections of the shank will reach the yield strength. Deformation (bending) of the coupler shank will increase and grow until equilibrium between external loads and internal resistance forces is reached, i.e., until the interaction of working surfaces, due to which the longitudinal force is transmitted, changes

TABLE 2. Calculated Values of the Longitudinal Force (MN)

Shank cross-section of the coupler	$e = \Delta h_a$ , cm	$e_y$ for the yield strength, cm		$e_y$ for the ultimate strength, cm	
		0	2	0	2
I-I	10	0.970	0.767	1.108	0.877
	8	0.965	0.765	1.103	0.974
	6	0.961	0.762	1.098	0.871
K-K	10	1.415	1.252	1.616	1.431
	8	1.384	1.228	1.582	1.404
	6	1.356	1.205	1.550	1.378

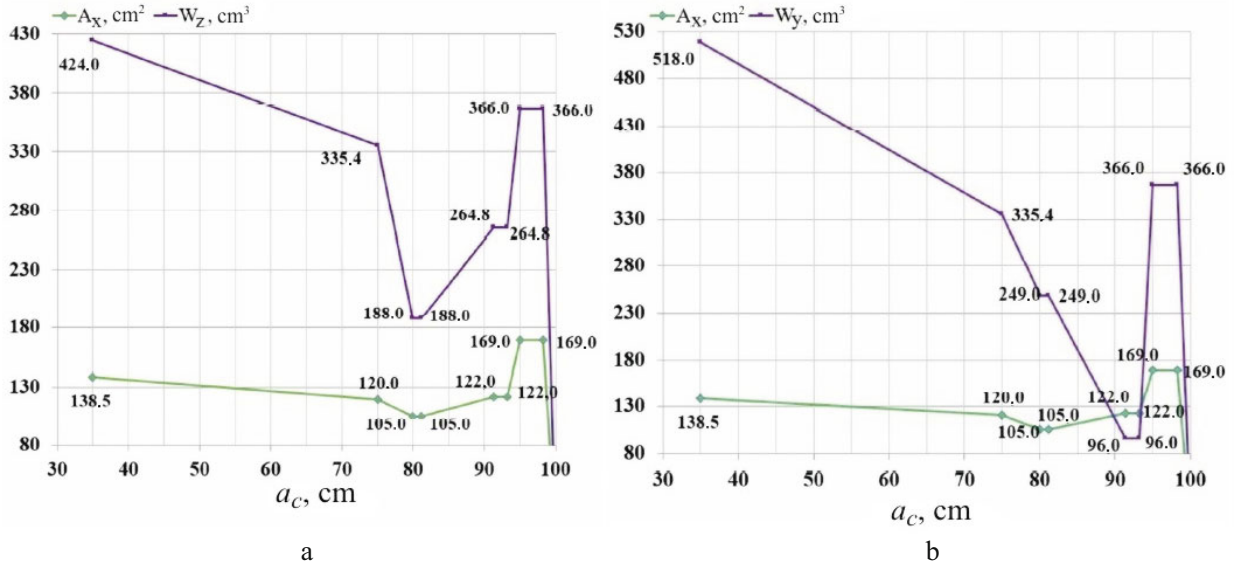


Fig. 7. Changes in the values of moments of resistance and cross-sectional area of the coupler shank along the length in the vertical (a) and in the horizontal (b) planes.

$$\sigma_{\max} = \frac{F}{A_x} + \frac{M_z(x)}{W_z(x)} + \frac{M_y(x)}{W_y(x)} \leq [\sigma_Y], \quad (6)$$

where  $[\sigma_Y]$  is the yield stress of the coupler shank material (Table 1).

In the process of modeling train movement and in the investigation of transport events, the values of longitudinal forces in the inter-car connections are used. Therefore, it is more convenient to use the longitudinal force value as a criterion for assessing the strength of the coupler body.

Solving together equations (2), (4), and (6), we find the longitudinal force  $F$  at the appearance of fluidity in the coupler shank

$$F = \frac{[\sigma_T]}{\frac{1}{A_x} + \frac{h_{xa}(a_c - x) - \Delta h_a x}{2a_c W_z(x)} + \frac{e_y(a_c - x) + e'_y a_c}{a_c W_y(x)}}. \quad (7)$$

In the derivation of equation (7), in order to obtain a simpler dependence for the vertical forces  $P_z$  and  $P_y$ , it was assumed that the moment of resistance of the considered section of the shank and the major axis of bending do not change when plastic deformation occurs, that is, the normal stress diagram during plastic deformation keeps the same shape as during elastic deformation; tangential stresses from vertical forces were also not taken into account.

**Discussion of the Results.** Substituting the values of yield strength  $[\sigma_Y]$  or ultimate strength  $[\sigma_u]$  for the coupler material (Table 1), as well as the values  $W_z(x)$ ,  $W_y(x)$ , and  $A_x$  for the weak sections  $I-I$  and  $K-K$  of the coupler shank (Fig. 7), we obtain the ultimate values of longitudinal force corresponding to the yield strength and ultimate strength. The results of the calculations are given in Table 2.

The results obtained show that in the case of non-central interaction of cars, if longitudinal forces are transmitted through the upper ribs of the end surface of the coupler shank, plastic deformation of the body in section  $I-I$  takes place at loads close to operating ones, and is 0.97 MN. Provided that the entire strain energy is taken up exclusively by the coupler body, the coupler does not meet the strength requirements.

**Conclusions.** There is an analysis of theoretical research into the determination of coupler body strength under the effect of compressive operating loads with regard to the non-central interaction of two cars. The calculation scheme takes into account that the compressive force is transferred to the coupler support plate in a point, which moves both in vertical and horizontal planes of the rail carriage. The effects of transverse and vertical eccentricity on the magnitude of compressive operating loads have been investigated. Theoretical research of the coupler's body strength in the presence of the transverse and vertical eccentricities of the longitudinal force application probably testifies that the damage of the coupler's shank jumper zone and the bending of the shank in horizontal and vertical planes, which are the most frequent damages of the coupler's body during the operation, appear not only because of the longitudinal forces and damping devices failures but also because of the change of the interaction direction. In the case of non-central interaction of the cars, if the longitudinal forces are transmitted through the upper ribs of the coupler shank end face, the plastic deformation of the body in  $I-I$  section takes place under the loads, which are close to the operating ones, and is almost 1 MN. This study has demonstrated the need to further elucidate in more detail the possible reasons, which cause changes in the direction of longitudinal forces transmission in the process of freight rolling stock operation.

The methodology of longitudinal force calculation allows to study the influence of eccentricities of its application in relation to the coupler axis and the difference of coupled coupler axis levels in the analyzed sections. The use of the obtained results will help not only to ensure the strength of the coupling devices, but also to increase the durability of freight cars under conditions of increasing train weight and speed of their movement.

## REFERENCES

1. M. Kurhan, D. Kurhan, and L. Černiauskaite, "Rationale of priority areas of rail operation in north-eastern Europe," in: Proc. of the 23rd Int. Sci. Conf. on Transport Means 2019, Lithuania, (2019), pp. 1439–1444.
2. M. Kurhan and D. Kurhan, "Providing the railway transit traffic Ukraine–European Union," *Pollack Periodica*, **14**, No. 2, 27–38 (2019), <https://doi.org/10.1556/606.2019.14.2.3>.
3. A. O. Shvets, "Determination of the stability of freight cars taking into account the railway track parameters," *Science and Transport Progress*, **2** (86), 103–118 (2020), <https://doi.org/10.15802/stp2019/195821>.
4. T. Zhu, B. Yang, C. Yang, et al., "The mechanism for the coupler and draft gear and its influence on safety during a train collision," *Vehicle Syst. Dyn.*, **56**, No. 9, 1375–1393 (2018), <https://doi.org/10.1080/00423114.2017.1413198>.
5. L. A. Muradyan, V. Yu. Shaposhnik, B. U. Vinstrot, and S. P. Mukovoz, "Tests of promising brake pads on the railways of Ukraine," *Lokomotiv-Inform*, Nos. 7–8, 20–22 (2015).
6. L. A. Muradian, V. Yu. Shaposhnyk, and A. A. Mischenko, "Methodological fundamentals of determination of unpowered rolling stock maintenance characteristics," *Science and Transport Progress*, **1** (61), 169–179 (2016), <https://doi.org/10.15802/stp2016/61044>.
7. L. A. Muradian, V. Yu. Shaposhnyk, and D. O. Podosenov, "Improving the reliability of freight wagons with the use of new manufacturing technologies and regeneration of working surfaces," *Electromagnetic Compatibility and Safety in Railway Transport*, No. 11, 49–54 (2016), <https://doi.org/10.15802/ecsrt2016/91337>.

8. V. Horobets, O. Sablin, E. Fedorov, et al., "Methods and results of evaluating the dual-power electric train crew elements service life," *IOP Conf. Ser.-Mat. Sci.*, **985**, 012028 (2020), <https://doi.org/10.1088/1757-899X/985/1/012028>.
9. K. Murawski, "Experimental comparison of the known hypotheses of the lateral buckling for semi-slender pinned columns," *Int. J. Struct. Glass Adv. Mater. Res.*, **5**, No. 1, 82–114 (2021), <https://doi.org/10.3844/sgamrsp.2021.82.114>.
10. A. A. Abdulhameed, A. N. Hanoon, H. A. Abdulhameed, and S. K. Mohaisen, "Energy absorption evaluation of CFRP-strengthened two-spans reinforced concrete beams under pure torsion," *Civil Eng. J.*, **5**, No. 9, 2007–2018 (2019), <https://doi.org/10.28991/cej-2019-03091389>.
11. E. P. Blokhin, K. I. Zheleznov, and L. V. Ursulyak, "Computing complex for solving the problems of safety and stability of the movement of rolling stock of railways," *Science and Transport Progress*, No. 18, 106–113 (2007).
12. A. O. Shvets, "Gondola cars dynamics from the action of longitudinal forces," *Science and Transport Progress*, **6** (84), 142–155 (2019), <https://doi.org/10.15802/stp2019/195821>.
13. A. O. Shimanovsky, P. A. Sakharau, and M. G. Kuzniatsova, "Research of the modern absorbing apparatus power characteristics influence on the freight train inter-car forces," *IOP Conf. Ser.-Mat. Sci.*, **985**, 012027 (2020), <https://doi.org/10.1088/1757-899X/985/1/012027>.
14. A. Shvets, O. Shatunov, S. Dovhaniuk, et al., "Coefficient of stability against lift by longitudinal forces of freight cars in trains," *IOP Conf. Ser.-Mat. Sci.*, **985**, 012025 (2020), <https://doi.org/10.1088/1757-899X/985/1/012025>.
15. A. A. Shvets, K. I. Zhelieznov, A. S. Akulov, et al., "Some aspects of the definition of empty cars stability from squeezing their longitudinal forces in the freight train," *Science and Transport Progress*, **4** (58), 175–189 (2015), <https://doi.org/10.15802/stp2015/49281>.
16. D. A. Juraev, "The solution of the ill-posed Cauchy problem for matrix factorizations of the Helmholtz equation," *Adv. Math. Model. Appl.*, **5**, No. 2, 205–221 (2020).
17. A. O. Shvets, "Stability of freight wagons under the action of compressing longitudinal forces," *Science and Transport Progress*, **1** (85), 119–137 (2020), <https://doi.org/10.15802/stp2020/199485>.
18. O. B. Kuzmin, V. S. Kossov, O. L. Protopopov, et al., "The strength research of the coupler parts during the exploitation downloading," *Science and Transport Progress*, No. 19, 170–175 (2007).
19. O. O. Nemchuk and O. A. Nesterov, "In-service brittle fracture resistance degradation of steel in a ship-to-shore portal crane," *Strength Mater.*, **52**, No. 2, 275–280 (2020), <https://doi.org/10.1007/s11223-020-00175-w>.
20. V. V. Kosarchuk, E. I. Danilenko, and A. V. Agarkov, "Effect of railcar wheel tire profiles on the contact stress level in subway rails," *Strength Mater.*, **52**, No. 3, 398–406 (2020), <https://doi.org/10.1007/s11223-020-00190-x>.
21. A. Ghosh and D. Chakravorty, "FEM analysis of progressive failure for composite hypar shells," *Strength Mater.*, **52**, No. 4, 507–520 (2020), <https://doi.org/10.1007/s11223-020-00202-w>.
22. V. Yu. Shaposhnyk, *Automatic Coupler Body*, Ukrtransakad, Dnepropetrovsk (2014).
23. D. V. Shevchenko, M. A. Kudryavtsev, A. M. Orlova, et al., "Numerical modeling of the dynamics of the clutch couplers," *Vestnik VNIIZhT*, **78**, No. 3, 155–161 (2019), <https://doi.org/10.21780/2223-9731-2019-78-3-155-161>.
24. S. V. Vershinsky, G. V. Kostin, A. D. Kochnov, and Yu. M. Cherkashin, "Investigation of the stability of the movement of freight cars in curves of small radius under the action of longitudinal stretching forces," *VNIIZhT Bulletin*, Issue 639, 11–23 (1981).